Hindawi Publishing Corporation
International Journal of Antennas and Propagation
Volume 2013, Article ID 345908, 6 pages
http://dx.doi.org/10.1155/2013/345908

*Research Article*

# Limits on Estimating Autocorrelation Matrices from Mobile MIMO Measurements

**Tricia J. Willink**

*Communications Research Centre Canada, P.O. Box 11490, Station H, 3701 Carling Avenue, Ottawa, ON, Canada K2H 8S2*

Correspondence should be addressed to Tricia J. Willink; tricia.willink@crc.gc.ca

Received 3 December 2012; Accepted 8 January 2013

Academic Editor: Pablo Padilla



On mobile radio links, data samples collected at successive time intervals and at closely spaced frequencies are correlated, so long data records are required to acquire sufficient independent samples for analysis. Statistical analysis of long data records is not reliable because the channel statistics remain wide-sense stationary only over short distances. This is a particular concern for MIMO systems when full autocorrelation matrices may be required for channel modelling or characterisation. MIMO channel responses from mobile measurements in an urban microcell have been used to investigate the limits on estimating autocorrelation matrices, and these are compared to those predicted by commonly used channel models.

## 1. Introduction

The effectiveness of the spatial processing that provides spectral efficiency gains in MIMO communication systems is dependent on the multipath structure of the channel, that is, the number, powers, and angles of the received multipath components. This structure is highly localised, so in a mobile environment the channel statistics change with time; in other words, the time series of complex channel responses between the transmitter and the receiver is not wide-sense stationary (WSS) except over short distances. This places limits on the length of the time series that can be used to analyse a particular channel characteristic. Within this short time series, there is a finite number of independent channel samples. In the analysis of measured data, therefore, it must be confirmed that there are sufficient independent samples to achieve a valid estimate of the characteristic of interest.

This work addresses the estimation of the full autocorrelation matrix of a MIMO channel. This autocorrelation matrix fully characterises the second order statistics of each of the transmitter-receiver pair links, giving a complete description of a Rayleigh fading MIMO channel; therefore, it has been used extensively in the characterisation and modelling of MIMO channels. For example, it has been applied to decompose the MIMO channel [1], to simulate a correlated MIMO channel [2], to estimate the double-directional angular power spectrum [3], and to evaluate the correlation [4] and diversity [5] of the MIMO channel.

The full autocorrelation matrix is computed using the outer product of channel vectors; hence, the number of independent samples must exceed the dimension of the channel vectors or the autocorrelation matrix estimate will necessarily be rank deficient. The size of the autocorrelation matrix that can be generated is therefore limited by the channel's time and frequency correlation properties as well as the wide-sense stationary interval and signal bandwidth. An important question is then what is the highest dimension mobile MIMO channel that can be characterised using measured data? To answer this, measured data obtained in a typical urban area have been analysed. The results are compared to those that would be obtained using commonly used channel models.

## 2. Autocorrelation Matrix Estimation

Consider a MIMO radio system with $N_t$ transmit antenna elements and $N_r$ receive antenna elements. The radio channel between transmit element $j$ and receive element $i$ is sampled at intervals $kT_s$ and is represented by the time-varying complex baseband impulse response $h_{ij}(k, \tau)$. The corresponding time-varying frequency transfer function at time $kT_s$ is $H_{ij}(k, n)$, defined at frequency indices $n\Delta f$, obtained as the

discrete Fourier transform of $h_{ij}(k,\tau)$ with respect to delay $\tau$. The $N_r \times N_t$ channel response matrix is then given by $\mathbf{H}(k,n)$, with elements $H_{ij}(k,n)$.

The sample autocorrelation matrix at a single frequency index, $n$, obtained over the time domain is

$$\widehat{\mathbf{R}}(n) = \frac{1}{N}\sum_{k=1}^{N} \operatorname{vec}(\mathbf{H}(k,n))\operatorname{vec}(\mathbf{H}(k,n))^H, \quad (1)$$

where vec denotes vectorisation of the matrix and ergodicity is assumed. At least $N_I = N_r \cdot N_t$ independent samples of $\mathbf{H}(k,n)$ are required to ensure that the estimate $\widehat{\mathbf{R}}(n)$ fully reveals the matrix rank: if there are insufficient independent samples, $\widehat{\mathbf{R}}(n)$ will be rank deficient even if the elements of $\mathbf{H}(k,n)$ are uncorrelated.

It is known from [6] that the channel statistics are unlikely to be WSS over distances of more than 2 m in an urban environment at 2 GHz. This can be considered to hold across the UHF band, as the locations of dominant reflecting objects in the local environment, that is, buildings, are the same and their sizes are on the order of many wavelengths, even at the lowest frequency. Estimating statistical functions of the channel response, such as the autocorrelation matrix, must therefore be restricted to intervals that are short enough to be considered WSS.

*2.1. Independent Samples.* Consider a WSS time series of $N$ samples at intervals $T_s$, with mean $\mu$ and variance $\sigma^2$. If the time series is uncorrelated, the variance of the sample mean is $\sigma_m^2 = \sigma^2/N$. However, when the time series is correlated, the variance of the sample mean increases as

$$\sigma_m^2 = \sigma^2 \sum_{k=-(N-1)}^{N-1} \frac{N-|k|}{N^2}\left(\rho(k) - \mu^2\right), \quad (2)$$

where $\rho(k)$ is the normalised correlation coefficient between samples separated by $kT_s$. It has been shown, for example, in [7, Ch. 5], that the variance of the sample mean does not vanish as $T_s$ increases if the overall duration of the time series remains the same.

As noted in [8, Ch. 3], the number of equivalent independent samples (EIS) in a time series of $N$ correlated samples can be determined by equating the variance of the sample mean to that of a time series of $N_I$ uncorrelated samples. The number of EIS is, therefore, given by

$$N_I = \frac{\sigma^2}{\sigma_m^2} = \left[\sum_{k=-(N-1)}^{N-1} \frac{N-|k|}{N^2}\left(\rho(k) - \mu^2\right)\right]^{-1}. \quad (3)$$

## 3. Measured Data

Mobile MIMO channel measurements were made in urban Ottawa using available frequency assignments at 2 GHz and 370 MHz, with sounding bandwidths of 25 MHz and 12.5 MHz, respectively. These frequencies are relevant for mobile communications, in particular, personal communications and emergency services and military applications, respectively. The transmitter was static, with $N_t = 4$ omnidirectional antenna elements arranged in a linear array, spaced at one wavelength for each frequency, and mounted at a height of approximately 3 m. The receiver was mobile and travelled at 30 km/h along a non-line-of-sight route that included intersections and the urban canyon between them. The $N_r = 4$ omnidirectional receiver antennas were mounted on the roof of the measurement van, also in a linear array of one-wavelength spacing with the axis perpendicular to the direction of travel, at a height of approximately 2 m. The location of the measurements is illustrated in Figure 1.

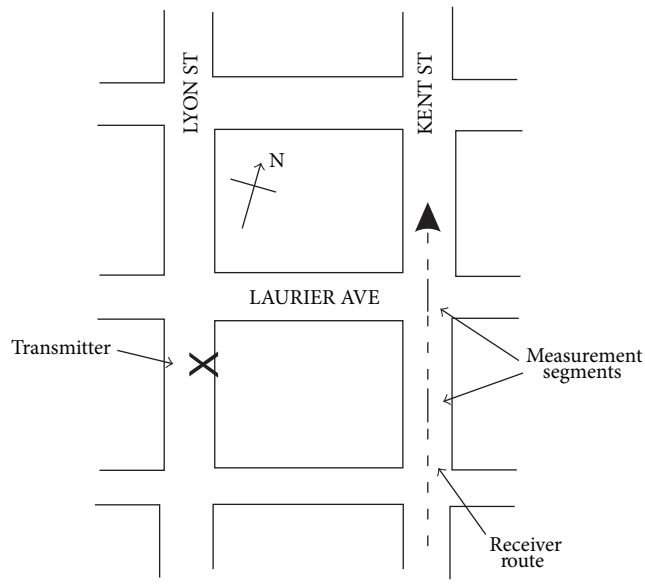


Figure 1: Location of measurement segments in downtown Ottawa, Canada.

The measurement system and the processing of sampled received data are described in [6]. The measured data yielded $N_r \cdot N_t = 16$ time series of channel impulse response estimates $h_{ij}(k,\tau)$ obtained at intervals of $T_s = 2$ ms, that is, distances of 0.017 m. Each was processed to give the channel transfer function estimates $H_{ij}(k,n)$. The central 20% of each frequency response was retained for analysis, and these frequency components were normalised to have the same average powers over the measurement run; this process retains only channel matrices that have a very high SNR and corrects the spectral shape of the modulated sounding sequence. Two segments of the time series were used, from a mid-block region and an intersection along the measurement route, each 2 s long.

## 4. Data Analysis

The time series for each measurement segment consisted of 1000 samples, and each was divided into subblocks of 120 samples (0.24 s), corresponding to the 2 m that can be considered WSS [6]. Mean-ergodicity was confirmed by considering the sample covariance, $C(l)$: for each measurement segment, in both the time and frequency dimensions, $(1/L)\sum_{l=0}^{L} C(l)(1 - l/2L)$ decreases monotonically to zero as

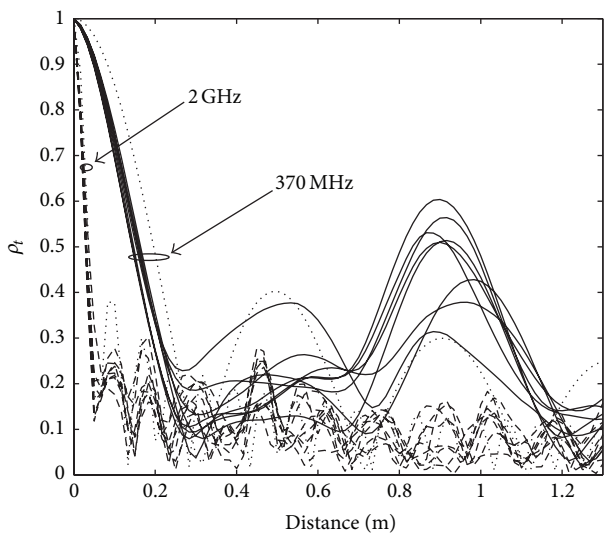


Figure 2: Spatially averaged temporal correlation function for the mid block region at 370 MHz (solid lines) and 2 GHz (dashed lines). The model correlation function at 30 km/hr is also shown (dotted lines).

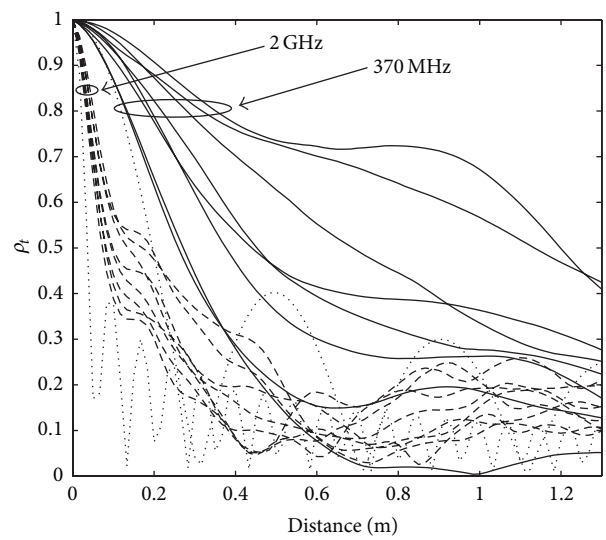


Figure 3: Spatially averaged temporal correlation function for the intersection region at 370 MHz (solid lines) and 2 GHz (dashed lines). The model correlation function at 30 km/hr is also shown (dotted lines).

$L$ is increased to the subblock length. The number of EIS in both time and frequency was investigated, as described below.

*4.1. Time Domain.* The normalised temporal correlation function estimates were computed for each of the $N_r \cdot N_t$ channel responses as follows:

$$\rho_t(l) = \frac{\mathscr{E}\left\{(H(k,n))(H(k+l,n))^*\right\}}{\mathscr{E}\left\{|H(k,n)|^2\right\}}, \tag{4}$$

where the subscripts on $H(k,n)$ have been dropped for convenience. The expectations were taken over the time and frequency dimensions of each subblock. The autocorrelation functions $\rho_t(l)$ were then averaged over the $N_r \cdot N_t = 16$ spatial channels.

Figures 2 and 3 show the space-averaged autocorrelation functions for the mid-block and intersection regions, respectively. The correlation function for the uniform scatterer model, with a Clarke Doppler power spectral density [9, Ch. 5], is also shown; that is,

$$\rho_t(\Delta t) = J_0\left(2\pi F_d \Delta t\right), \tag{5}$$

where $J_0$ is the zeroth order Bessel function of the first kind and $F_d$ is the maximum Doppler frequency. At 30 km/hr, $F_d = 55.6$ Hz at 2 GHz and 10 Hz at 370 MHz. In the mid-block region, the measured correlation functions vary only a small amount over each of the eight 2 m long subblocks, whereas there is considerable variation in the intersection. The measured data in the mid-block region is also better represented by the model, although the accuracy is not high. This is because the model is based on the assumption of many multipath components arriving with random amplitudes and uniformly distributed angles of arrival. In practice, within an urban canyon, the strongest multipath components arrive from angles close to the front and/or rear of the vehicle, and not from the sides [6]. In the intersection, as seen in [10], the signal power arrives predominantly from the side, along the direction of the intersecting street, with some reflections off the buildings on opposite corners. These directional components lead to higher temporal correlations and greater variation from subblock to subblock as the angles of arrival change with distance.

The number of EIS was obtained by applying (3) to the correlation function computed for each subblock and averaging. The results are shown in Figure 4 for each frequency and region, along with the number of EIS expected when using the idealised model (5). As expected, the number of EIS is larger at the higher frequency, as the correlation function decreases more rapidly with delay or distance. The average number of EIS is greater in the mid-block region than in the intersection, but none of the measured data provide the number of EIS predicted by the model. As noted above, the spatial characteristics of the observed multipath are not matched by the assumptions in the model.

The asymptotic behaviour is of particular significance. While the model predicts an increase in EIS of 1.75 per 10 ms at 2 GHz and 0.33 per 10 ms at 370 MHz, for the measured data the observed EIS increases are approximately 0.1–0.2 per 10 ms at 2 GHz and 0.05–0.15 per 10 ms at 370 MHz. This is because $\rho_t(l)$ is much greater for large delays, $l$, than predicted by the model, as shown in Figures 2 and 3, which significantly reduces $N_I$ (3).

*4.2. Frequency Domain.* The normalised frequency correlation function estimates were estimated for each subblock and for each element in the channel matrix time series using

$$\rho_f(m) = \frac{\mathscr{E}\left\{(H(k,n))(H(k,n+m))^*\right\}}{\mathscr{E}\left\{|H(k,n)|^2\right\}} \tag{6}$$

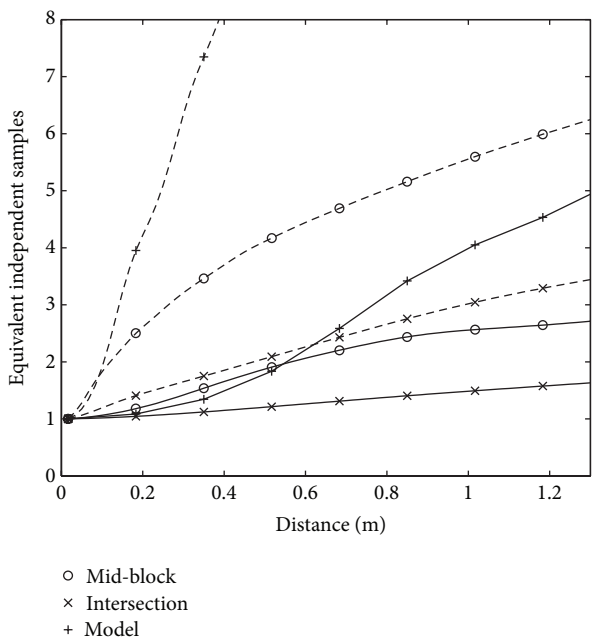


Figure 4: Average equivalent independent samples for time-correlated data at 30 km/hr for 370 MHz (solid lines) and 2 GHz (dashed lines) and for the Clarke Doppler model (5).

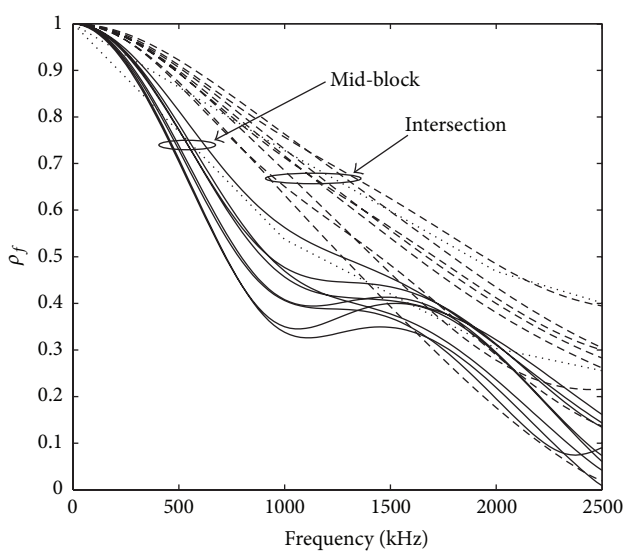


Figure 5: Spatially averaged frequency correlation function at 2 GHz for the mid-block region (solid lines) and the intersection (dashed lines). The model correlation functions for $\tau_0 = 0.25\,\mu$s and $\tau_0 = 0.15\,\mu$s are also shown (dotted lines).

and were then averaged over the $N_r \cdot N_t = 16$ spatial channels. The necessity to the average over time as well as frequency when computing a frequency correlation estimate was pointed out in [11], as a single snapshot in time represents only one relationship of multipath phases and amplitudes. The variation across the subblocks is quite small, as shown in Figure 5 for the 2 GHz measurements, and is similar for both frequencies and regions.

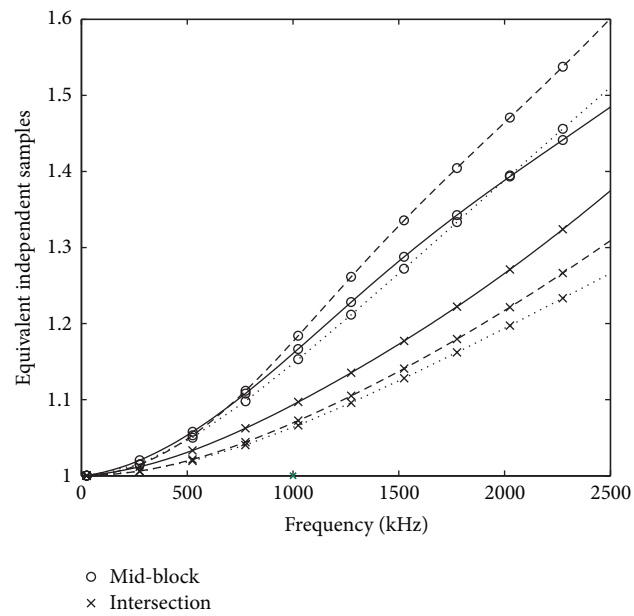


Figure 6: Average equivalent independent samples for frequency-correlated data at 370 MHz (solid lines) and 2 GHz (dashed lines) and for exponential delay model (7) (dotted lines).

The number of EIS was then computed for each subblock using (3), and the average is shown in Figure 6 for each frequency and region. The figure also shows the number of EIS computed for the exponential delay profile model [9, Ch. 7], which has the correlation function

$$\rho_f(\Delta f) = \left(1 + j2\pi\tau_0\Delta f\right)^{-1}, \tag{7}$$

where $\tau_0$ is the root-mean-square delay spread. From the measured data, $\tau_0$ was estimated to be $0.25\,\mu$s in the mid-block region and $0.15\,\mu$s in the intersection. The computed model correlation functions are shown in Figure 5.

The numbers of EIS over the bandwidths considered here, which are limited by the measurement bandwidth, are very small. At both 370 MHz and 2 GHz, the number of EIS per bandwidth is greater in the mid-block region where a richer multipath environment results in a larger delay spread and therefore a reduced correlation across the channel bandwidth.

The measured channel impulse responses do not follow a simple exponential delay profile but are better modelled using multiple clusters of multipath components, as described in [9, Ch. 7]. In spite of this, the simple and tractable exponential delay profile model, using an appropriate rms delay spread parameter, does provide a good estimate of the EIS. This is because the rms delay spread is strongly related to the frequency correlation, and the parameterisation of $\tau_0$ leads to a reasonably representative correlation function even if the delay profile itself is not accurately represented, as shown in Figure 5. The EIS for the measured data slightly exceed those of the model, because the measured correlation function (Figure 5) tends to decay faster than that of the model; however, this simple model does lead to similar asymptotic

behaviour, with measurements and model predicting an increase of approximately 0.15–0.25 EIS per 1000 kHz.

## 5. Discussion

The analysis of measured data indicates that the full autocorrelation matrix, $\mathbf{R}$, can be generated only for a small number of antenna elements in urban environments. The main limitation is the distance over which the time series of channel responses can be considered to be WSS. This distance has been estimated to be approximately 2 m in the type of environment considered here. The time correlation model that is usually considered, with a Clarke Doppler power spectral density, indicates that there are approximately 8 and 42 independent samples in 2 m, at 30 km/hr, for 370 MHz and 2 GHz, respectively. For a MIMO system with $N_r = N_t$, the autocorrelation matrix can then be estimated for maximum array sizes of 2 and 6, respectively.

The impact of insufficient independent samples is illustrated in Figure 7, which shows the average estimated diversity, using the diversity metric proposed in [5]. The narrowband channel is modelled using $N_t = N_r = 4$, $R_{ii} = 1$, and $R_{ij} = \rho$, for $i \neq j$, for $i, j = 1, \ldots, 16$, using a Clarke fading model at a carrier frequency of 2 GHz and a speed of 30 km/hr. The diversity metric is given by [5]

$$\Phi = \frac{\left[\sum_{i=1}^{N_t \cdot N_r} \lambda_i\right]^2}{\sum_{i=1}^{N_t \cdot N_r} \lambda_i^2}, \tag{8}$$

where $\lambda_i$, $i = 1, \ldots N_t \cdot N_r$, are the eigenvalues of the autocorrelation matrix estimate $\widehat{\mathbf{R}}$ in (1), and the channel is sampled at intervals $T_s = 5$ ms. For the spatially uncorrelated channel, the diversity is significantly underestimated for distances even up to 8 m. This deficit is reduced as the spatial correlation increases, but even for $\rho = 0.3$, there are not enough independent samples in a measurement length of 2 m to fully reveal the rank of $\widehat{\mathbf{R}}$, resulting in an underestimation of the diversity by approximately one unit.

In practice, the assumptions of rich, uniformly distributed scattering are not met in this urban environment. The number of equivalent independent samples over 2 m is actually observed to be between 3 and 4 at 370 MHz and between 6 and 9 at 2 GHz. The richer multipath scattering environment of the mid-block region provides more EIS than that in the intersection, where there is a small number of dominant multipath components.

The frequency domain does not provide much to supplement the number of EIS. For a measurable bandwidth of 10 MHz, less than 3 EIS are achieved, depending on the local environment. At 100 MHz, based on the exponential power delay profile model, this would increase from 10 to 16 EIS, which is sufficient to estimate arrays with $N_r = N_t = 4$ in a mid-block region, but not in an intersection. In [12], measurements with $N_t = N_r = 4$ were reported for a bandwidth of 240 MHz, at a carrier frequency of 5.2 GHz; the analysis presented herein indicates that averaging over a bandwidth that large would certainly provide sufficient independent samples to generate the full autocorrelation matrix,

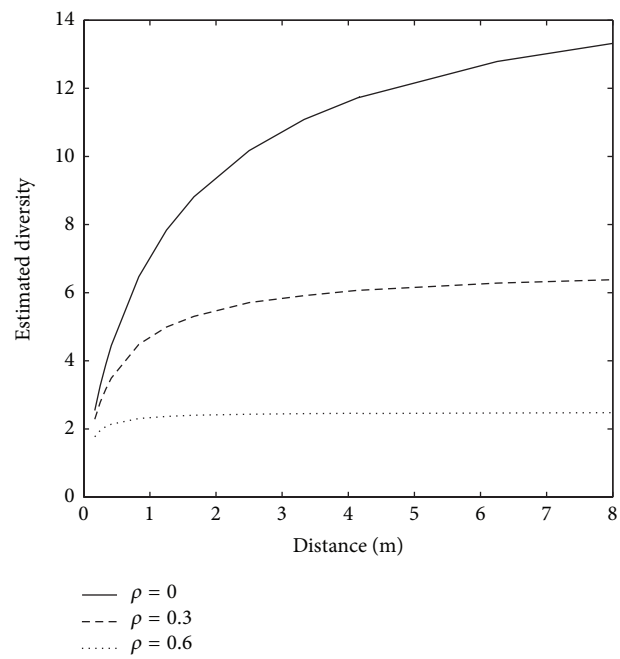


Figure 7: Estimated diversity (8) for correlated fading model at 30 km/hr for 2 GHz.

assuming a typical urban delay profile. The higher frequency also enables more independent samples to be obtained over the same measurement distance than for the 2 GHz results reported herein. Obtaining such a large spectrum assignment for measurements, especially at lower frequencies, can be difficult, so in general care must be taken to ensure that the bandwidth used does indeed provide enough equivalent independent samples such that the autocorrelation matrix will not necessarily be rank deficient.

For the measurements presented, combining both time and frequency domains for a measurable bandwidth of 2 MHz and distance of 2 m at 30 km/hr, the autocorrelation matrix $\mathbf{R}$ cannot be generated for more than $N_r = N_t = 2$ at 370 MHz nor for more than $N_r = N_t = 3$ at 2 GHz. Note that this only ensures the estimated autocorrelation matrix is not rank deficient, as analysed [13, Ch. 5]; the accuracy of the estimate also depends on the number of independent samples.

## 6. Conclusions

The analysis of mobile MIMO measurement data reported herein has shown that the estimation of the full autocorrelation matrix, $\mathbf{R}$, should be restricted to small numbers of antenna elements due to the limited number of independent samples in a typical wide-sense stationary interval. Estimating $\mathbf{R}$ with too few independent samples will prevent its full rank from being revealed. If the channel bandwidth is very large and the channel's delay spread is sufficiently large; that is, it has a sufficiently small correlation bandwidth, averaging the autocorrelation matrix across the bandwidth as well as in time will help supplement the number of equivalent

independent samples. The number of EIS is dependent on the local environment as well as operating frequency, with more EIS in the mid-block region than in the intersection. Conventional fading models do not provide good estimates of EIS for localised measurements because the assumptions used in their derivations are often not satisfied, but it has been seen that simple delay profile models may be more useful if appropriately parameterised.

## References


[1] W. Weichselberger, "On the decomposition of the MIMO channel correlation tensor," in *Proceedings of the ITG Workshop on Smart Antennas*, pp. 268–273, March 2004.

[2] J. P. Kermoal, L. Schumacher, K. I. Pedersen, P. E. Mogensen, and F. Frederiksen, "A stochastic MIMO radio channel model with experimental validation," *IEEE Journal on Selected Areas in Communications*, vol. 20, no. 6, pp. 1211–1226, 2002.

[3] H. Özcelik, N. Czink, and E. Bonek, "What makes a good MIMO channel model?" in *Proceedings of the IEEE 61st Vehicular Technology Conference (VTC '05)*, vol. 1, pp. 156–160, Stockholm, Sweden, May 2005.

[4] D. S. Shiu, G. J. Foschini, M. J. Gans, and J. M. Kahn, "Fading correlation and its effect on the capacity of multielement antenna systems," *IEEE Transactions on Communications*, vol. 48, no. 3, pp. 502–513, 2000.

[5] M. Ivrlač and J. Nossek, "Quantifying diversity and correlation in Rayleigh fading MIMO communication systems," in *Proceedings of the 3rd IEEE International Symposium on Signal Processing and Information Technology (ISSPIT '03)*, pp. 158–161, December 2003.

[6] T. J. Willink, "Wide-sense stationarity of mobile MIMO radio channels," *IEEE Transactions on Vehicular Technology*, vol. 57, no. 2, pp. 704–714, 2008.

[7] W. B. Davenport and W. L. Root, *An Introduction to the Theory of Random Signals and Noise*, McGraw-Hill, 1958.

[8] F. E. Nathanson, J. P. Reilly, and M. N. Cohen, *Radar Design Principles: Signal Processing and the Environment*, SciTech Publishing, 1999.

[9] A. F. Molisch, *Wireless Communications*, John Wiley & Sons, 2005.

[10] C. C. Squires and T. J. Willink, "Impact of vehicular array position on urban MIMO channel characteristics," *International Journal of Antennas and Propagation*, vol. 2011, Article ID 675343, 14 pages, 2011.

[11] R. J. C. Bultitude, "Estimating frequency correlation functions from propagation measurements on fading radio channels: a critical review," *IEEE Journal on Selected Areas in Communications*, vol. 20, no. 6, pp. 1133–1143, 2002.

[12] A. Paier, T. Zemen, J. Karedal et al., "Spatial diversity and spatial correlation evaluation of measured vehicle-to-vehicle radio channels at 5.2 GHz," in *Proceedings of the IEEE 13th Digital Signal Processing Workshop*, pp. 326–330, January 2009.

[13] Y. Eldar and G. Kutyniok, Eds., *Compressed Sensing, Theory and Applications*, Cambridge University Press, 2012.